We are IntechOpen,
the world's leading publisher of
Open Access books
Built by scientists, for scientists

6,900
Open access books available

186,000
International authors and editors

200M
Downloads

154
Countries delivered to

Our authors are among the

TOP 1%
most cited scientists

12.2%
Contributors from top 500 universities

CLARIVATE ANALYTICS
BOOK CITATION INDEX
INDEXED

WEB OF SCIENCE™

Selection of our books indexed in the Book Citation Index
in Web of Science™ Core Collection (BKCI)

Interested in publishing with us?
Contact book.department@intechopen.com

Numbers displayed above are based on latest data collected.
For more information visit www.intechopen.com

Simultaneous Topology, Shape and Sizing Optimisation of Skeletal Structures Using Multiobjective Evolutionary Algorithms

Chaid Noilublao and Sujin Bureerat

Applied Mathematics and Optimisation Research Unit, Department of Mechanical Engineering, Faculty of Engineering, Khon Kaen University, 4000 Thailand

1. Introduction

A framework or skeletal structure is one of the most used structures in engineering applications. Using such a structure is said to be advantageous since they are simple and inexpensive to construct. It can be employed in many engineering purposes e.g. transmission towers, wind turbine towers, communication towers, civil engineering structures, and mechanical parts. In the past, the design of such a structure was usually carried out in such a way that the conceptual design stage was somewhat ignored and the initial shape of a structure had been formed by an experienced engineering designer. The classical civil engineering design approach is then applied in the preliminary and detailed design stages.

Recently topology optimisation, an efficient tool for structural conceptual design, has been studied and used in a wide range of engineering applications. Considerable research work on the conceptual design of truss and frame structures by means of topology optimisation has been conducted in the last two decades (e.g. Hajela & Lee,1995; Ohsaki, 1995; Zhou, 1996; Yunkang & Xin, 1998; Hasancebi & Erbatur, 2002; Kawamura et al., 2002; Stolpe & Svanberg, 2003; Ohsaki & Katoh, 2005; Achtziger & Stolpe, 2007; Svanberg & Werme, 2007; Hagishita & Ohsaki, 2009). By the use of such design technology, the optimised layout of a skeletal structure can be accomplished. Having a structural layout from this design process, the shape and sizing design processes are then implemented. Nevertheless, a more efficient design approach can be achieved if a design problem is posed to have topological, shape, and sizing design variables at the same time. Much research work has been conducted towards combining and performing topology, shape, and sizing optimisation at the same optimisation run (e.g. Wang et al., 2004; Zhou et al., 2004; Tang et al., 2005; Shea & Smith, 2006; Achtziger, 2007; Martínez et al., 2007; Chan & Wong, 2008; Noiluplao & Bureerat, 2008; Zhu et al., 2008). The optimum design problem of the simultaneous topology/shape/sizing optimisation is usually structural weight minimisation subject to stress and other safety constraints. The optimisers employed can be a derivative-based method (Martínez et al., 2007), an evolutionary algorithm (Tang et al., 2005; Shea & Smith, 2006; Noiluplao & Bureerat, 2008), and a hybrid method (Chan & Wong, 2008). From the literature, most if not all of the optimisation problems are formulated to have one objective function, whereas in a

practical design of an engineering system, there usually are several design objectives for decision making. If we have an optimiser that can deal with the design problem with such multiple design objectives, it could be useful and beneficial for designers.

Evolutionary algorithms (EAs) have been developed and used for several decades. The methods can be viewed as optimisation methods that search for optimum solutions by imitating some kinds of natural behaviours, and relying on a random process. Most EA searches are based upon using a population or a group of design solutions; consequently, they are often called population-based optimisers. Compared to their gradient-based counterparts, the EAs have advantages in that their searching process can be performed without using function derivatives. The methods are robust and simple to use, and can deal with almost all kinds of optimum design problems. As they are dependent on randomisation, EAs however have some drawbacks since they have low convergence rates and lack search consistency.

Evolutionary algorithms can deal with both single- and multiple-objective optimisation problems. The best known single-objective evolutionary optimiser is the genetic algorithm. Some other established single-objective EAs are: evolution strategies, particle swarm optimisation, and population-based incremental learning. EAs that can deal with multiple objective functions are called multiobjective evolutionary algorithms (MOEAs). As they use a set of design solutions for searching, on each generation those solutions can be sorted to find the so-called non-dominated design solutions. The set of non-dominated design solutions are improved iteratively, and the final set is taken as an approximate Pareto optimal set. This is the most outstanding and attractive ability of MOEAs as they can search for a group of non-dominated design solutions within one optimisation run. While the other conventional gradient-based optimisers need to be run as many times as the number of Pareto optimal solutions required.

The use of EAs for structural optimisation has been investigated and studied by many researchers around the world. By using EAs, any kind of design variables, constraints, as well as objective function can be defined. With additional strong points i.e. the capability of reaching near global optima of EAs and their robustness, they are even more popular than their gradient-based counterparts. The methods can be used for structural weight or cost minimisation (Benage & Dhingra, 1994, Bureerat & Cooper, 1988), passive vibration alleviation (Keane, 1995; Ton et al., 1998; Moshrefi-Torbati et al., 2003; Alkhatib et al., 2004; Kanyakam & Bureerat, 2007), and other performance maximisation (Xu et al., 2003; Achtziger & Kocvara, 2007).

The work in this chapter, consisting of two parts, is concerned with the demonstration of implementing MOEAs on the optimisation of skeletal structures. In the first part, the performance comparison of a number of MOEAs including non-dominated sorting genetic algorithm (NSGAII), strength Pareto evolutionary algorithm (SPEA2), population-based incremental learning (PBIL), Pareto archive evolution strategy (PAES), and multiobjective particle swarm optimisation (MPSO) are employed to solve seven simultaneous shape and sizing design problems of two structures. The comparative studies are carried out by using the so-called *C*-indicator. Also, a new indicator *C′* is proposed to be used along with the *C* parameter. The Pareto optimum results obtained from using the various MOEAs are compared and discussed while some of the best performers are obtained. The second part involves the application of MOEAs to a simultaneous topology/shape/sizing optimisation of a skeletal structure. The design demonstrations are performed and illustrated.

2. Multiobjective evolutionary algorithms

A typical multiobjecitve optimisation problem can be defined as:

find **x** such that

$$\text{Min: } \mathbf{f} = \{f_1(\mathbf{x}),\ldots,f_m(\mathbf{x})\} \tag{1}$$

Subject to

$$g_i(\mathbf{x}) \leq 0$$
$$h_i(\mathbf{x}) = 0$$

where **x** is a vector of n design variables, f_i are the m objective functions, g_i are inequality constraints, and h_i are equality constraints.

If the problem has one objective, there will be one (global) optimum solution. In cases that the problem has more than one objective function, there will be a set of optimal solutions, which is called a Pareto optimum set. Figure 1 illustrates a particular 2-objective design problem where all the feasible solutions are plotted in the objective domain. The Pareto optimal solutions are the points on the bold frontier, which is called a Pareto frontier or Pareto front. Similarly to the 2-objective case, the Pareto front of a 3-objective design problem is a 3-dimensional surface and so on.
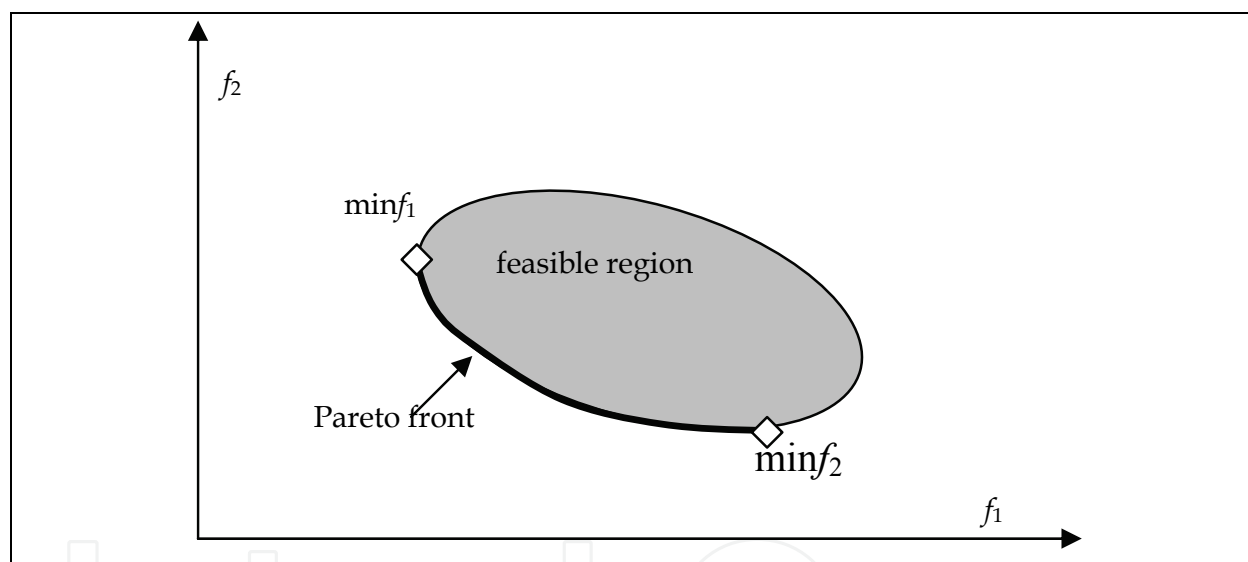

Fig. 1. Pareto front

The basic concept of exploring Pareto optimum points via MOEA search is that, in each generation while a new population is created, non-dominated solutions are classified and carried on to the next generation. The term non-dominated solutions define the local Pareto solutions among the members of the current population during evolutionary search. The definitions associated with non-domination (for minimisation) are given as:

Definition 1 **Dominance** Given $f_i(\mathbf{x})$ for $i = 1,\ldots m$ are objective functions, if $f_i(\mathbf{x}_1) \leq f_i(\mathbf{x}_2)$ for every $i \in \{1,\ldots,m\}$ and there is j such that $f_j(\mathbf{x}_1) < f_j(\mathbf{x}_2)$, then $\mathbf{x}_1$ dominates $\mathbf{x}_2$.

Definition 2 **Non-Dominated Solutions** (**Approximate Pareto Set**) Given a set of solutions or population **G** size N, a solution $\mathbf{x}_e \in \mathbf{G}$ is a non-dominated solution in **G** if there does not exist $\mathbf{x} \in \mathbf{G}$ such that $\mathbf{x}$ dominate $\mathbf{x}_e$.

Figure 2 displays the plot of 7 design solutions on a 2-objective domain. The non-dominated solutions are $\mathbf{x}_1$, $\mathbf{x}_3$, and $\mathbf{x}_7$.
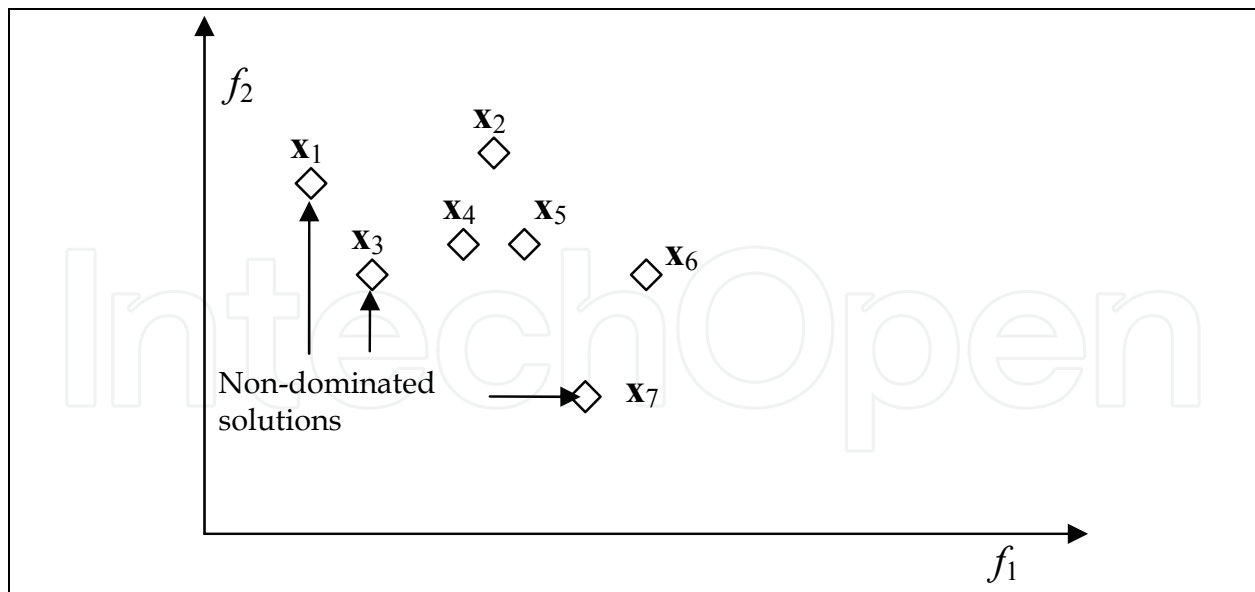
Fig. 2. non-dominated solutions

In this work, five MOEAs are used including PAES, NSGAII, SPEA2, PBIL and MPSO. The methods are briefly reviewed as follows:

2.1 Pareto archive evolution strategy

PAES was proposed by Knowles & Corne, 2000. The simplest version of PAES is the combination of (1+1)-ES with a Pareto archiving strategy. The algorithm starts with an initial solution called a parent and an external Pareto archive. A candidate solution is then created by mutating the parent. The parent will be replaced by the candidate based on a selection strategy. The decision to discard or add the candidate to the Pareto archive is made. In cases that the archive is full, the adaptive grid algorithm is activated to remove one of the non-dominated solutions from the archive. As the procedure continues, the Pareto archive is iteratively updated until reaching the termination criterion.

2.2 Non-dominated sorting genetic algorithm

NSGA was proposed by Srinivas & Deb, 1994, and later the upgraded version NSGAII was presented by Deb et al., 2002. Starting with an initial population, selection, crossover and mutation operators are then used for exploring Pareto solutions. After crossover and mutation are operated with the given probabilities, the children are obtained and a new population is selected by performing non-dominated and crowding distance sorting algorithms on a union set of the parents and their children. The population is updated iteratively until the termination criterion is met.

2.3 Strength Pareto evolutionary algorithm

SPEA was proposed by Zitzler & Thiele, 1999, whereas its second version SPEA2 was presented in Zitzler et al., 2002. The search procedure starts with an initial population and an external Pareto set. Fitness values are assigned to the population based upon the level of domination. A set of solutions are then selected to a mating pool by performing the binary tournament selection operator. The new population are created by means of crossover and mutation on those selected solutions. The new external Pareto solutions are the non-

dominated solutions of the combination of the old external Pareto set and the new population. In cases that the number of non-dominated solutions in the Pareto archive exceeds its predefined size, the truncation operator also known as the nearest neighbourhood technique is executed to delete some design solutions from the archive. The Pareto archive is updated repeatedly until the termination criterion is met.

2.4 Multiobjective particle swarm optimisation

The particle swarm optimisation method uses real codes and searches for an optimum by mimicking the movement of a flock of birds, which aim to find food (Reyes-Sierra & Coello Coello, 2006). The search procedure herein is based on the particle swarm concepts combining with the use of an external Pareto archiving scheme. Starting with an initial set of design solutions as well as their corresponding particle velocities and objective function values, an initial Pareto archive is filled with the non-dominated solutions obtained from sorting the initial population. A new population is then created by using the particle swarm updating strategy where the global best solution is randomly selected from the external Pareto archive. Afterwards, the external archive is updated by the non-dominated solutions of the union set of the new population and the previous non-dominated solutions. In cases that the number of non-dominated solutions is too large, the adaptive grid algorithm (Knowles & Corne, 2000) is employed to properly remove some solutions from the archive. The Pareto archive is repeatedly improved until fulfilling the termination criteria.

2.5 Population-based incremental learning

Population-based incremental learning, probably the simplest form of an estimation of distribution algorithm (EDA), was first proposed by Beluja, 1994, for single-objective optimisation. The method was then extended for multiobjective optimisation (Bureerat & Sriworamas, 2007; Kanyakam & Bureerat, 2007). The algorithm of multiobjective PBIL starts with an external Pareto archive and initial probability matrix having all elements set to be 0.5. A set of binary design solutions are then created corresponding to the probability matrix while their function values are evaluated. The Pareto archive is updated by replacing its members with the non-dominated solutions of the new population and the previous Pareto archive. In cases that the number of non-dominated solutions exceeds the predefined archive size, the normal line method is activated to remove some members from the archive. The probability matrix and the Pareto archive are iteratively updated until the termination criteria are fulfilled.

3. Structural modelling

A structural dynamic model can be described as a structure being in a dynamic equilibrium state. It is the state at which the system has minimum potential energy (potential energy herein includes structural elastic potential energy, the work done by external forces, and the work due to inertial forces). The equations of motion basically comprise of kinetic energy, structural restoration (spring and damping) and external dynamic forces. By using the finite element approach, the structural dynamic model is represented by

$$\mathbf{M}\ddot{\boldsymbol{\delta}} + \mathbf{K}\boldsymbol{\delta} = \mathbf{F}(t) \tag{2}$$

where $\boldsymbol{\delta}$ is the vector of structural displacements, **M** is a structural mass matrix, **K** is a structural stiffness matrix, and **F** is the vector of dynamic forces acting on the structure.

The computation is traditionally achieved by means of finite element analysis. With the given boundary conditions (say $\boldsymbol{\delta}_b = \mathbf{0}$) being given, Equation (2) can be partitioned as

$$\begin{bmatrix} \mathbf{M}_{aa} & \mathbf{M}_{ab} \\ \mathbf{M}_{ba} & \mathbf{M}_{bb} \end{bmatrix} \begin{bmatrix} \ddot{\boldsymbol{\delta}}_a \\ \ddot{\boldsymbol{\delta}}_b \end{bmatrix} + \begin{bmatrix} \mathbf{K}_{aa} & \mathbf{K}_{ab} \\ \mathbf{K}_{ba} & \mathbf{K}_{bb} \end{bmatrix} \begin{bmatrix} \boldsymbol{\delta}_a \\ \boldsymbol{\delta}_b \end{bmatrix} = \begin{bmatrix} \mathbf{F}_a \\ \mathbf{F}_b \end{bmatrix} \tag{3}$$

where the subscript *b* indicates the known displacements and unknown reactions at the boundary conditions, and the subscript *a* denotes unknown displacements and predefined external forces.

Equation (3) can be rearranged leading to 2 systems of differential equations as:

$$\mathbf{M}_{aa}\ddot{\boldsymbol{\delta}}_a + \mathbf{K}_{aa}\boldsymbol{\delta}_a = \mathbf{F}_a \tag{4}$$

and

$$\mathbf{M}_{ba}\ddot{\boldsymbol{\delta}}_a + \mathbf{K}_{ba}\boldsymbol{\delta}_a = \mathbf{F}_b . \tag{5}$$

In the cases of free vibration analysis, Equation (4) can be written as

$$\mathbf{M}_{aa}\ddot{\boldsymbol{\delta}}_a + \mathbf{K}_{aa}\boldsymbol{\delta}_a = \mathbf{0} . \tag{6}$$

By substituting $\boldsymbol{\delta}_a = \overline{\boldsymbol{\delta}}_a e^{i\omega t}$ to (6), we have an eigenvalue problem

$$(\mathbf{K}_{aa} - \omega^2 \mathbf{M}_{aa})\overline{\boldsymbol{\delta}}_a = \mathbf{0} . \tag{7}$$

Solving such a system of equations leads to N natural frequencies $\boldsymbol{\omega} = \{\omega_1, \omega_2, \ldots, \omega_N\}$ and their corresponding eigenvectors $\boldsymbol{\Phi} = [\boldsymbol{\varphi}_1, \boldsymbol{\varphi}_2, \ldots, \boldsymbol{\varphi}_N]$, where N is the size of the square mass and stiffness matrices. The orthogonality conditions can be written as

$$\boldsymbol{\Phi}^T \mathbf{M}_{aa} \boldsymbol{\Phi} = diag(\mu_i) \tag{8}$$

$$\boldsymbol{\Phi}^T \mathbf{K}_{aa} \boldsymbol{\Phi} = diag(\mu_i \omega_i^2) . $$

By using the proportional (Rayleigh) damping concept, a damping matrix can be introduced to the model yielding

$$\mathbf{M}_{aa}\ddot{\boldsymbol{\delta}}_a + \mathbf{C}_{aa}\dot{\boldsymbol{\delta}}_a + \mathbf{K}_{aa}\boldsymbol{\delta}_a = \mathbf{F}_a \tag{9}$$

where $\mathbf{C}_{aa} = \alpha\mathbf{M}_{aa} + \beta\mathbf{K}_{aa}$, and α and β are damping coefficients to be defined.

From equation (9), by substituting $\boldsymbol{\delta}_a = \overline{\boldsymbol{\delta}}_a e^{i\omega t}$ and $\mathbf{F}_a = \overline{\mathbf{F}}_a e^{i\omega t}$, a frequency response function (FRF) matrix can be determined from the relation (Preumont, 2001)

$$\mathbf{H}(\omega) = \left[-\omega^2\mathbf{M}_{aa} + j\omega\mathbf{C}_{aa} + \mathbf{K}_{aa}\right]^{-1} = \boldsymbol{\Phi} diag\left\{\frac{1}{\mu_i(\omega_i^2 - \omega^2 + 2j\xi_i\omega_i\omega)}\right\}\boldsymbol{\Phi}^T \tag{10}$$

where ω is the frequency of the input force and its output displacement, and $\xi_i = \frac{1}{2}\left(\frac{\alpha}{\omega_i} + \beta\omega_i\right)$ is a damping ratio. FRF can be defined as the ratio of steady-state harmonic output to steady-state harmonic input, and here is the ratio of response displacement to input force or *receptance*. To reduce computational time in the optimisation process, the frequency response function matrix can be approximated using the first m modes as (Preumont, 2001)

$$\mathbf{H}(\omega) \approx \sum_{i=1}^{m} \frac{\boldsymbol{\varphi}_i \boldsymbol{\varphi}_i^T}{\mu_i(\omega_i^2 - \omega^2 + 2j\xi_i\omega_i\omega)} + \mathbf{K}_{aa}^{-1} - \sum_{i=1}^{m} \frac{\boldsymbol{\varphi}_i \boldsymbol{\varphi}_i^T}{\mu_i\omega_i^2} . \tag{11}$$

The relation between displacement response and input force can be expressed as

$$\overline{\boldsymbol{\delta}}_a = \mathbf{H}(\omega)\overline{\mathbf{F}}_a . \tag{12}$$

Figure 3 illustrates how to measure $H(r,s)$ which represents the ratio of a displacement response at the rth degree of freedom to a harmonic excitation at the sth degree of freedom. Furthermore, by defining force transmissibility (FT), denoted by $\mathbf{T}(\omega)$, as the ratio of output harmonic reaction forces to the input external harmonic forces, it can be written as

$$\overline{\mathbf{F}}_b = \mathbf{T}(\omega)\overline{\mathbf{F}}_a . \tag{13}$$
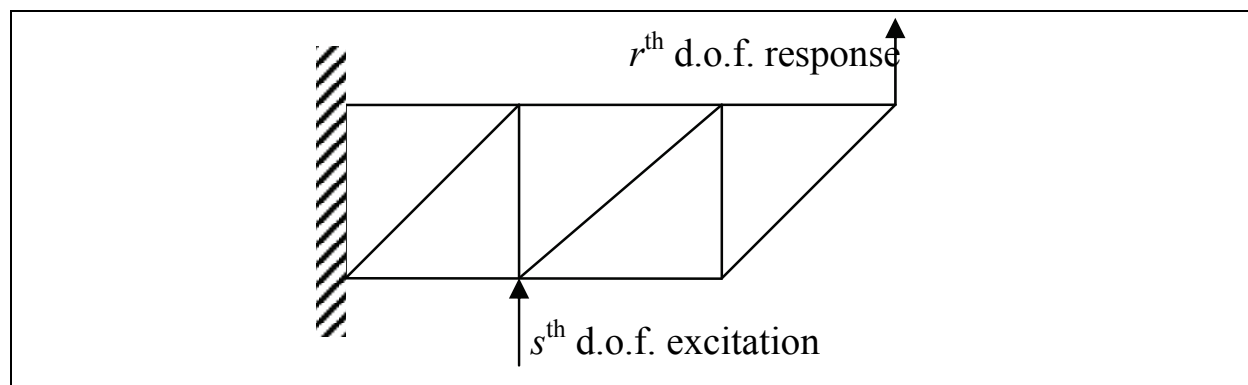
Fig. 3. Measurement of FRF

By letting the reaction force be $\mathbf{F}_b = \overline{\mathbf{F}}_b e^{i\omega t}$, and substituting (12) & (13) in (5), force transmissibility can be obtained as

$$\mathbf{T}(\omega) = \left(-\omega^2\mathbf{M}_{ba} + \mathbf{K}_{ba}\right)\mathbf{H} . \tag{14}$$

In structural vibration design, FRF and FT determine structural merit. The lower FRF or FT at a particular frequency means the better structural vibration suppression design. Therefore, a design objective can be assigned in such a way that frequency responses at a frequency range of interest are minimised. Moreover, maximising structural natural frequency is an alternative criterion for design of structures under dynamic loadings.

Apart from dynamic analysis, structural static analysis can be carried out by using Equation (3) ignoring the structural kinetic energy or the mass matrix. The system of equations then becomes

$$\begin{bmatrix} \mathbf{K}_{aa} & \mathbf{K}_{ab} \\ \mathbf{K}_{ba} & \mathbf{K}_{bb} \end{bmatrix} \begin{bmatrix} \boldsymbol{\delta}_a \\ \boldsymbol{\delta}_b \end{bmatrix} = \begin{bmatrix} \mathbf{F}_a \\ \mathbf{F}_b \end{bmatrix}. \tag{15}$$

The solutions of (15) are

$$\boldsymbol{\delta}_a = \mathbf{K}_{aa}^{-1}(\mathbf{F}_a - \mathbf{K}_{ab}\boldsymbol{\delta}_b) \tag{16}$$

and

$$\mathbf{F}_b = \mathbf{K}_{ba}\boldsymbol{\delta}_a - \mathbf{K}_{bb}\boldsymbol{\delta}_b. \tag{17}$$

The displacement vector $\boldsymbol{\delta}$ is used for displacement constraints as well as for computing stresses on structural elements. The reaction $\mathbf{F}_b$ is also an important factor since the reaction force can affect a structural foundation. In an optimisation process, it is also common to use many load cases since, in real-world problems, there are many aspects of applied loads acting on one structure.

4. Numerical experiment

4.1 Design problems
The optimisation problems assigned in this study are to find a Pareto optimal set that optimises multiple objective functions subject to stress constraints, which can be expressed as

$$\min_{\mathbf{x}} \mathbf{f} \tag{18}$$

subject to

$$\sigma_i \le \sigma_a, \ i = 1, \dots, N_e$$

where σ_i is a stress on the ith element, σ_a is an allowable stress, and N_e is the total number of elements.

The multiobjective design problems presented here are similar to the work in Kanyakam & Bureerat, 2007, where the objective functions include structural mass, a natural frequency, an FRF crest parameter, and an FT crest parameter. Figure 4 displays the term FRF crest parameter, which determines the shaded area in a frequency range of interest. As we need
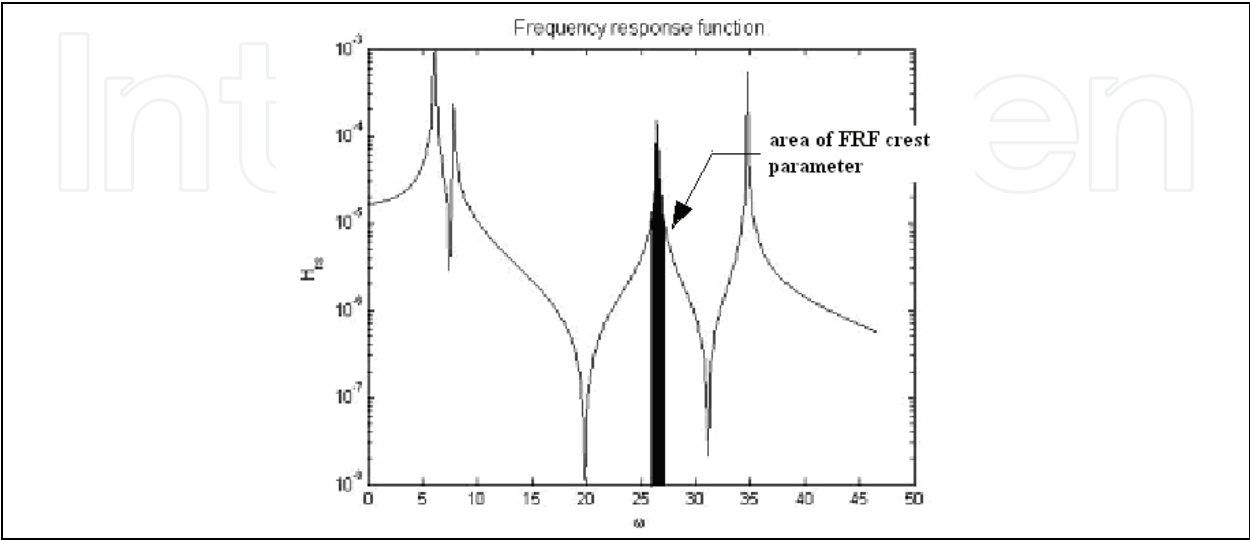

Fig. 4. FRF crest parameter

to reduce the magnitude of the FRF for vibration suppression, the frequency range is thus the interval that bounds a particular natural frequency. Seven design criteria are defined as:

f_1: structural mass

f_2: $1/\omega_1^2$

f_3: $1/(\omega_1^2 + \omega_2^2 + \omega_3^2)$

f_4: FRF crest parameter at ω_1

f_5: mean value of FRF crest parameters at ω_1, ω_2 and ω_3

f_6: FT crest parameter at ω_1

f_7: mean value of FT crest parameters at ω_1, ω_2 and ω_3

where ω_i is the ith natural frequency.

The sets of objective functions can be arranged as:

P1: min f_1, min f_2

P2: min f_1, min f_3

P3: min f_1, min f_4

P4: min f_1, min f_5

P5: min f_1, min f_6

P6: min f_1, min f_7

P7: min f_1, min f_5, min f_7.

As a result, we have seven multiobjective design problems with the above sets of objective functions and stress constraints. It should be noted that some of these objective function sets have been implemented and examined in Kanyakam & Bureerat, 2007, and it is shown that using P2, P4 and P6 leads to a more effective design based on vibration alleviation. All seven design problems are however used to benchmark the performance of the MOEAS.

We apply the above-mentioned problems to design three frame structures made of material with $E = 209{\times}10^9$ N/m², and $\rho = 7000$ kg/m³. The structures are named as:

ST1: a 2D bridge (Figure 5). The structure has 12 nodes and 21 elements where nodes 1 and 12 are fixed. The vertical loads are applied to nodes 2, 4, 6, 8, and 10. The design variables consist of element diameters, and the vertical positions of nodes 3, 5, 7, 9, and 11. Both shape and sizing design variables are treated as being symmetric; as a result, there are 14 continuous design variables. The FRF used as design criteria is the point receptance in the vertical direction of node 7. The FT is the vertical direction transmission from node 7 to the fixed support node 1.
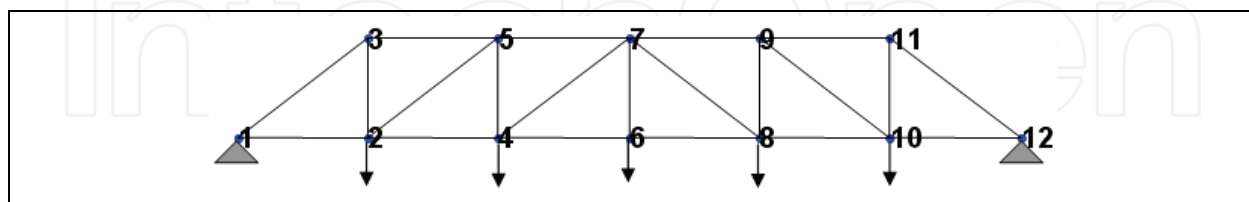

Fig. 5. 2D bridge ST1

ST2: a walking tractor handlebar (Figure 6). The finite element model of the handlebar structure (Kanyakam & Bureerat, 2007) consists of 16 nodes and 27 elements with four nodes being fixed. The structure is subjected to two static load cases, one is the load for turning the tractor and the other is the load for balancing and controlling the tractor. The total number of continuous shape and sizing design variables is 24. The FRF being used is the point receptance in the vertical direction of node 6. The FT is the vertical direction transmission from node 6 to the fixed support node 1.
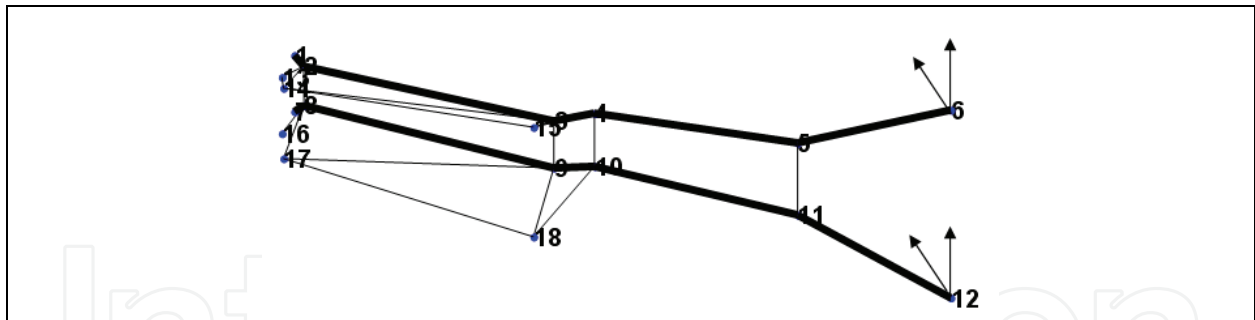
Fig. 6. Walking tractor handlebar structure ST2

ST3: a 2D bridge (Figure 7). The ST3 structure is modified from ST1 for the demonstration of simultaneous topology/shape/sizing optimisation. The structure in Figure 7, which is set as a ground structure for topology optimisation, has 12 nodes and 25 elements. The design variables are element diameters, and the vertical and horizontal positions of nodes 3, 5, 7, 9, and 11, which have a total of 18 variables after symmetry treatment. The diameters are discrete and allowed to have nearly zero size so that we can have various structural topologies. The position of FRF and FT measures are the same as that of ST1.

Finite element analysis is carried out by using the 2-node 3-dimensional 12 d.o.f. beam element. The ST1 and ST2 structures are used for the investigation of a comparative performance of MOEAs, while the ST3 structure is assigned for the demonstration of performing topology/shape/sizing optimisation at the same time.
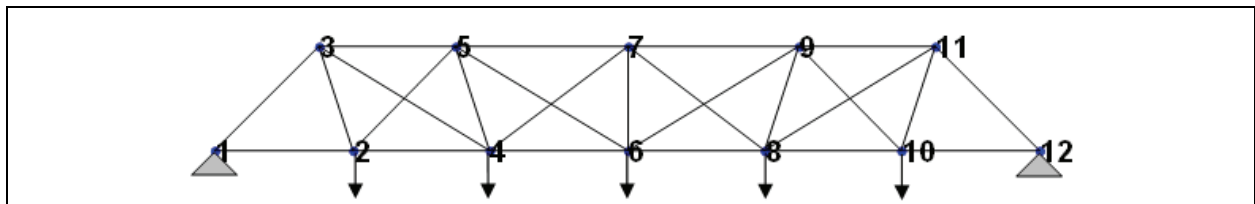
Fig. 7. 2D bridge's ground structure for simultaneous topology/shape/sizing optimisation ST3

4.2 Performance assessment

Seven multiobjective evolutionary strategies are employed in this study, which are designated as:

BPBIL: PBIL using binary codes with 0.05 mutation rate, and 0.2 mutation shift

BPAES: PAES using binary codes

BNSGA: NSGAII using binary codes with crossover and mutation rates as 1.0 and 0.5 respectively

BSPEA: SPEA2 using binary codes with crossover and mutation rates as 1.0 and 0.5 respectively

RSPEA: SPEA2 using real codes (Sirsomporn & Bureerat, 2008) with crossover and mutation rates as 1.0 and 0.5 respectively

RNSGA: NSGAII using real codes with crossover and mutation rates as 1.0 and 0.5 respectively

RMPSO: MPSO (Reyes-Sierra & Coello Coello, 2006) using real codes with a starting inertia weight, an ending inertia weight, a cognitive learning factor, and a social learning factor as 0.5, 0.01, 0.5, and 0.5 respectively.

For the comparative performance study of optimising ST1 and ST2, starting with the same initial population, the number of generations of MOEAs is set to be 100 while both the population and archive size are set as 50. Each optimiser is applied to solve each design problem for designing each structure with 10 optimisation runs. The last updated Pareto archive is set to be a Pareto optimal set. For the design of ST3, one of the best MOEAs obtained from the first two design case studies is employed to solve the P2, P4, and P6 design problems with the number of generations being 150 while the population and the external archive are sized 100. The non-dominated sorting scheme proposed in Deb et al. (2001) is used to handle the stress constraints.

The performance assessment is accomplished by using the C-parameter (Zitzler et al., 2000). Having two particular non-dominated fronts $\{A\}$ and $\{B\}$, $C_{A,B}$ determines the number of solutions in $\{B\}$ that are dominated or equal to some solution in $\{A\}$ divided by the total number of solutions in $\{B\}$. On the other hand, $C_{B,A}$ determines the number of solutions in $\{A\}$ that are dominated or equal to some solution in $\{B\}$ divided by the total number of solutions in $\{A\}$. From the definition, if $C_{A,B} > C_{B,A}$, we can say that front $\{A\}$ is better than front $\{B\}$ or vice versa. Figure 8 displays two approximate Pareto fronts $\{A\}$ and $\{B\}$ where $C_{A,B} = 0.5000$ and $C_{B,A} = 0.4000$. This implies that $\{A\}$ is better than $\{B\}$. However, we can observe from the shaded areas between the two fronts dominating each other that the dominating area of $\{B\}$ is larger than $\{A\}$. These shaded areas are also meaningful for front comparison. Nevertheless, it is difficult or even impossible to calculate such areas of hundred pairs of Pareto fronts directly. We can laterally calculate them and define a new performance indicator as:

$$C'_{A,B} = \frac{V_A}{V_A + V_B} \tag{19}$$

$$C'_{B,A} = 1 - C'_{AB}$$

where

$$V_A = \sum_{\mathbf{a} \in \hat{A}_1} \min \left\{ \|\mathbf{a} - \mathbf{b}\|; \mathbf{b} \in \hat{B}_1 \right\}$$

and

$$V_B = \sum_{\mathbf{b} \in \hat{B}_2} \min \left\{ \|\mathbf{b} - \mathbf{a}\|; \mathbf{a} \in \hat{A}_2 \right\}.$$

If $V_A = V_B = 0$, $C'_{A,B} = C'_{B,A} = 0.5$.

$\hat{A}_1$ is the set of some members of $\{A\}$ that dominate the set of $\hat{B}_1 \subseteq \{B\}$ and $\hat{B}_2$ is the set of some members of $\{B\}$ that dominate $\hat{A}_2 \subseteq \{A\}$. Similarly to the C parameter, if $C'_{A,B} > C'_{B,A}$, it means $\{A\}$ is better than $\{B\}$. From the definition, the C'-indicator also has the effects of front extension and the number of dominant points.

From Figure 8, we have $C'_{A,B} = 0.4556$ and $C'_{B,A} = 0.5444$, which means $\{B\}$ is the better front than $\{A\}$. Based on these two indicators, we have two different views of comparing approximate Pareto fronts. The special characteristic of the C' parameter is illustrated in Figure 9, which shows three particular non-dominated fronts $\{A_1\}$, $\{A_2\}$, and $\{A_3\}$. The C and

C' comparisons of the three fronts are given in Table 1. In the Table, the value in the ith row and jth column represents $C_{Ai,Aj}$. From the C comparison, it can be concluded that the front $\{A_3\}$ is the best method while the second best is $\{A_1\}$. However, in cases of C' comparison, we can see that $\{A_2\}$ is better than $\{A_1\}$, $\{A_1\}$ is better than $\{A_3\}$, and $\{A_3\}$ is better than $\{A_2\}$. This scenario can be called a scissor-paper-stone situation, which can happen in comparing approximate Pareto fronts obtained from using MOEAs. The two indicators, in fact, are not always conflicting to each other but they should be used together to provide different aspects of front comparing.
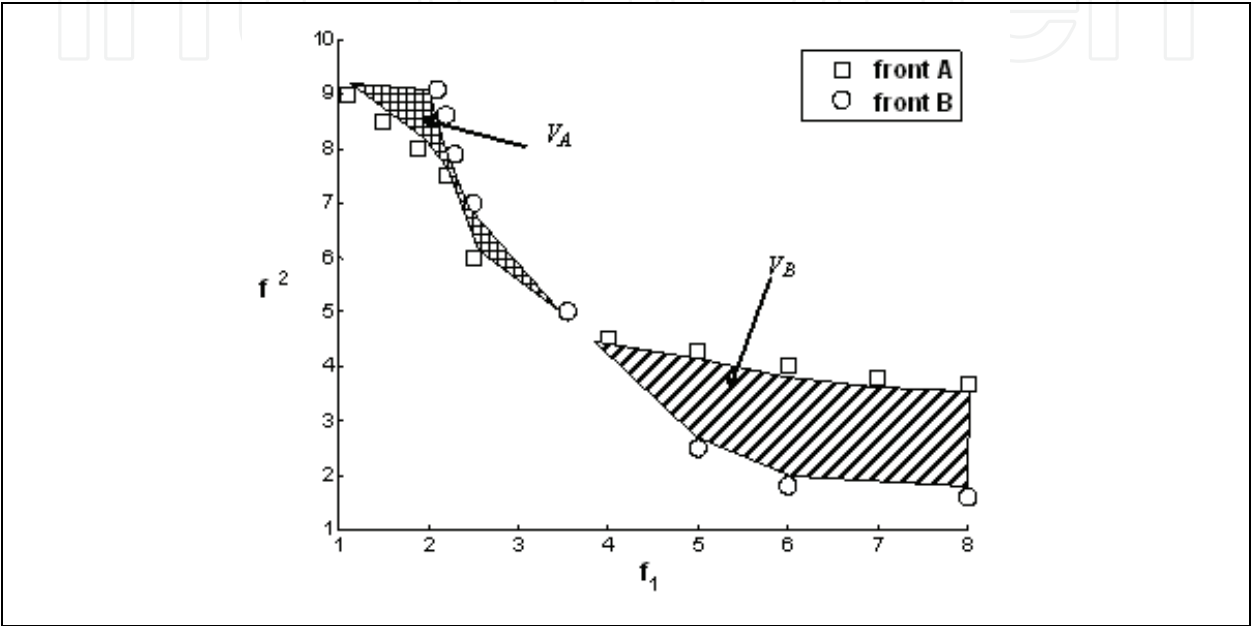
Fig. 8. Comparing two non-dominated fronts
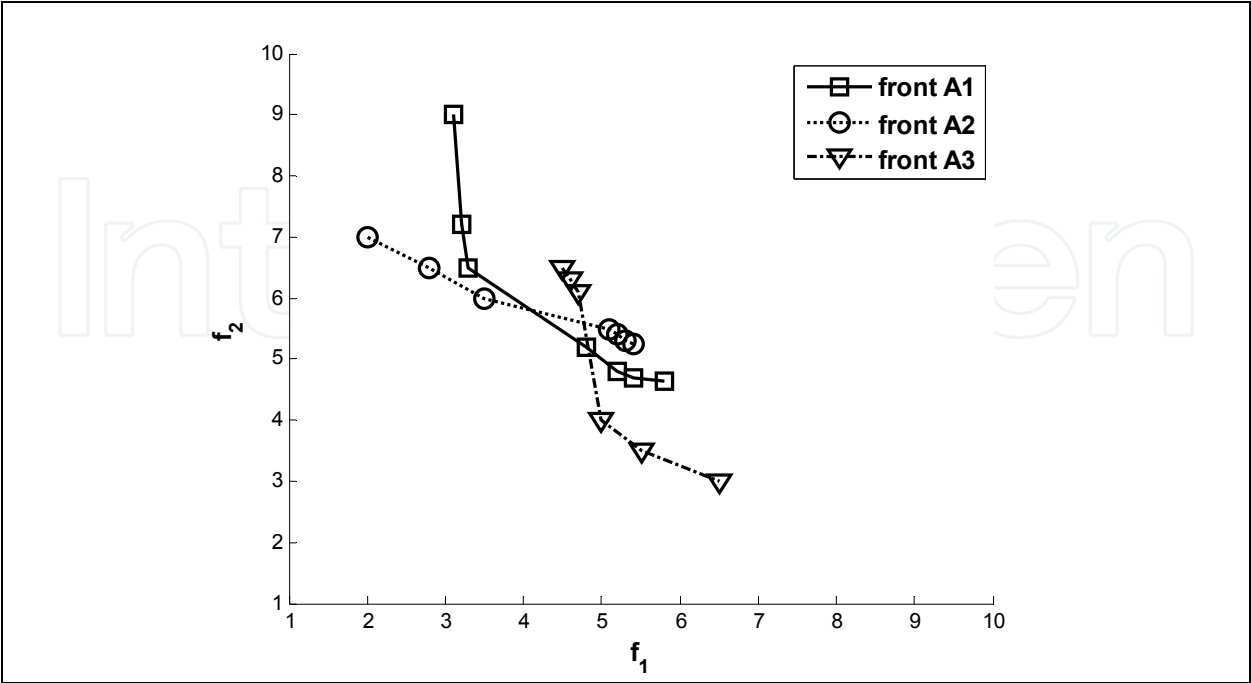
Fig. 9. Scissors-paper-stone situation

C-indicator			C'-indicator		
$\{A_1\}$	0.5714	0.1667	$\{A_1\}$	0.4929	0.5029
0.4286	$\{A_2\}$	0.5000	0.5076	$\{A_2\}$	0.4908
0.4286	0.5714	$\{A_3\}$	0.4971	0.5092	$\{A_3\}$

Table 1. C and C' indicators of $\{A_1\}$, $\{A_2\}$, and $\{A_3\}$

5. Design results

The performance comparison of 7 MOEAs is displayed in Figures 10 – 17. In Figure 10, the box-plots of C parameters comparing the various MOEAs when solving the P1-P7 design problems for the case of ST1 are illustrated. Each box-plot represents 10×10 C values of comparing 10 fronts obtained from using a method X to 10 fronts obtained from using a method Y when solving a particular design problem. The box-plots at the ith row and jth column display the C values comparing non-dominated fronts of the seven design problems obtained from the ith optimiser with respect to those obtained from using the jth optimiser. For example the box-plots at the first row and second column in the figure present the C values of the fronts obtained from using BNSGA to those obtained from using BSPEA. We also need the box-plots in the second row and first column to compare these two optimisers. From the Figure, it can be concluded that BPBIL is the best for all the design problems. The C' comparison of these four methods is given in Figure 11. It can be shown that BPBIL is the best method except for the P7 design problem, which BNSGA gives the best results.

The best multiobjective evolutionary algorithm using binary codes BPBIL is taken to be compared with the methods using real codes as shown in Figures 12-13. From the C comparison in Figure 12, the overall best method is BPBIL with RSPEA being the second best. In Figure 13, it can be seen that RSPEA is as good as BPBIL based on C' comparison. This occurrence is probably similar to that illustrated in Figure 8. However, when taking an account of both indicators, the best method for designing ST1 is BPBIL.
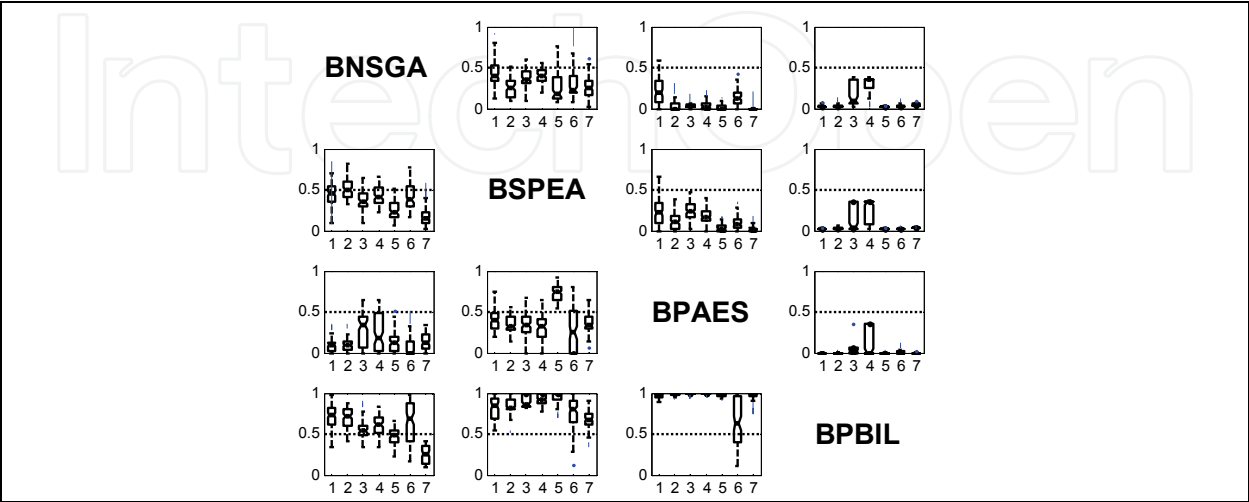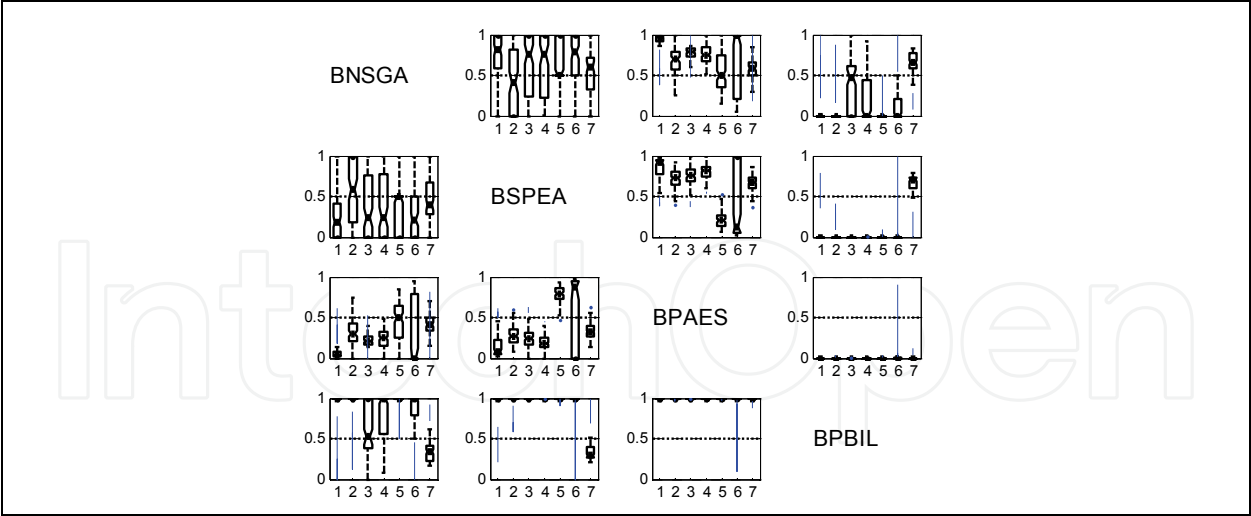

Fig. 10. Box-plot of C indicator of ST1 – I

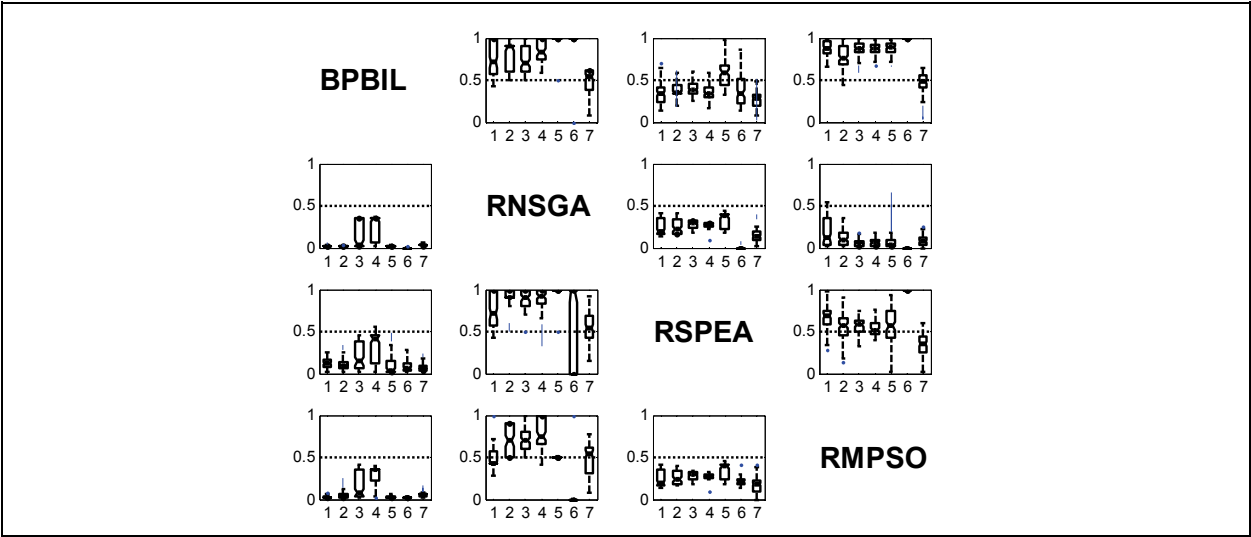Fig. 11. Box-plot of C' indicator of ST1 – I

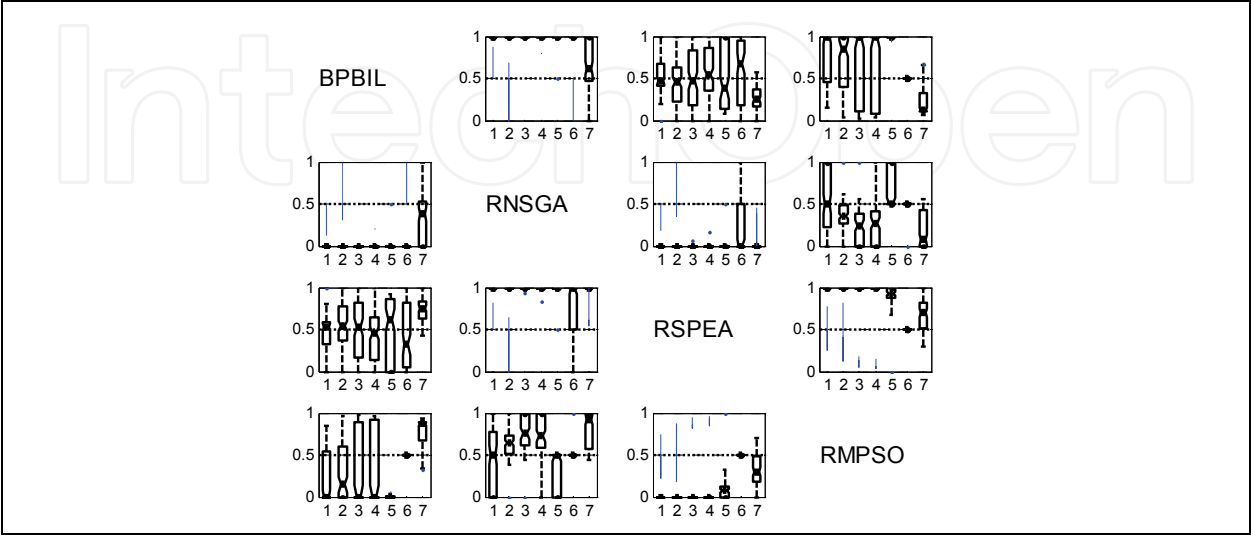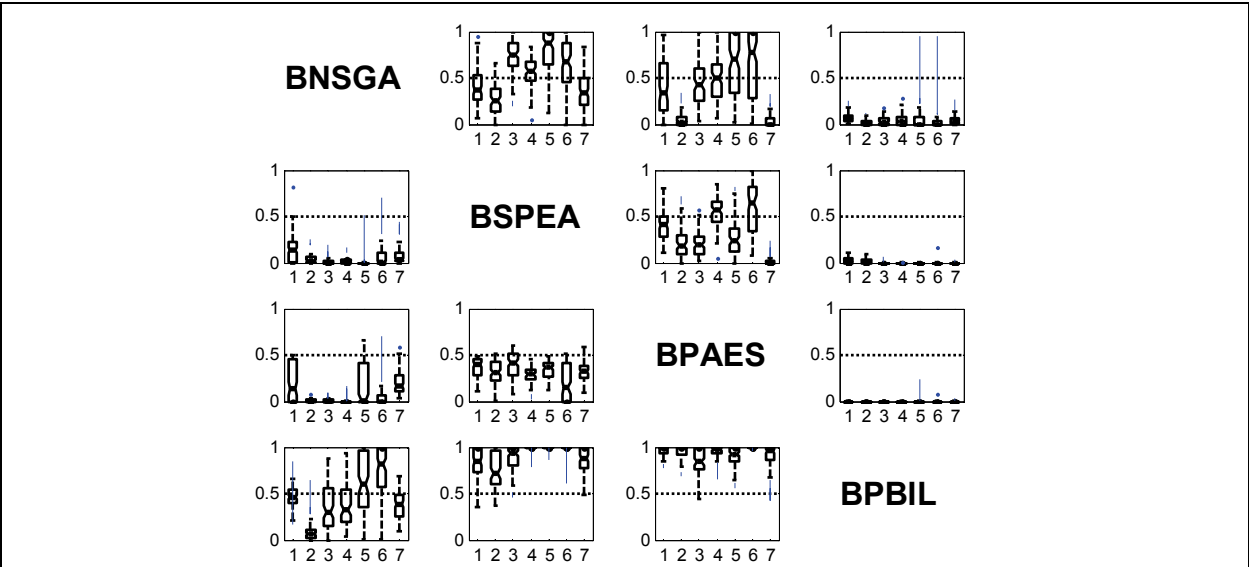Fig. 12. Box-plot of C indicator of ST1 – II

Fig. 13. Box-plot of C' indicator of ST1 - II

The comparative performance of MOEAs for solving the P1-P7 optimisation problems for the case of ST2 is illustrated in Figures 14-17. The best method that use binary codes based on the C indicator is BPBIL whereas the second best method is BNSGA as shown in Figure 14. Based on the C' indicator, the best method is BPBIL while the close second best is BNSGA. BNSGA even outperforms BPBIL in cases of the P3 and P4 design problems. This situation is similar to that displayed in Figure 8.

The best evolutionary optimiser among the methods using binary codes (BPBIL) is taken to be compared with the optimisers using real codes as shown in Figures 15 and 16. Based on the C indicator, the best optimiser is RSPEA whereas the second best is BPBIL. For the C' comparison, the best optimiser is still RSPEA with BPBIL being the second best. From both ST1 and ST2 case studies, it can be concluded that BPBIL tends to be more efficient when dealing with design problems with a smaller number of design variables while RSPEA is the better optimiser for the design problems with a greater number of design variables.

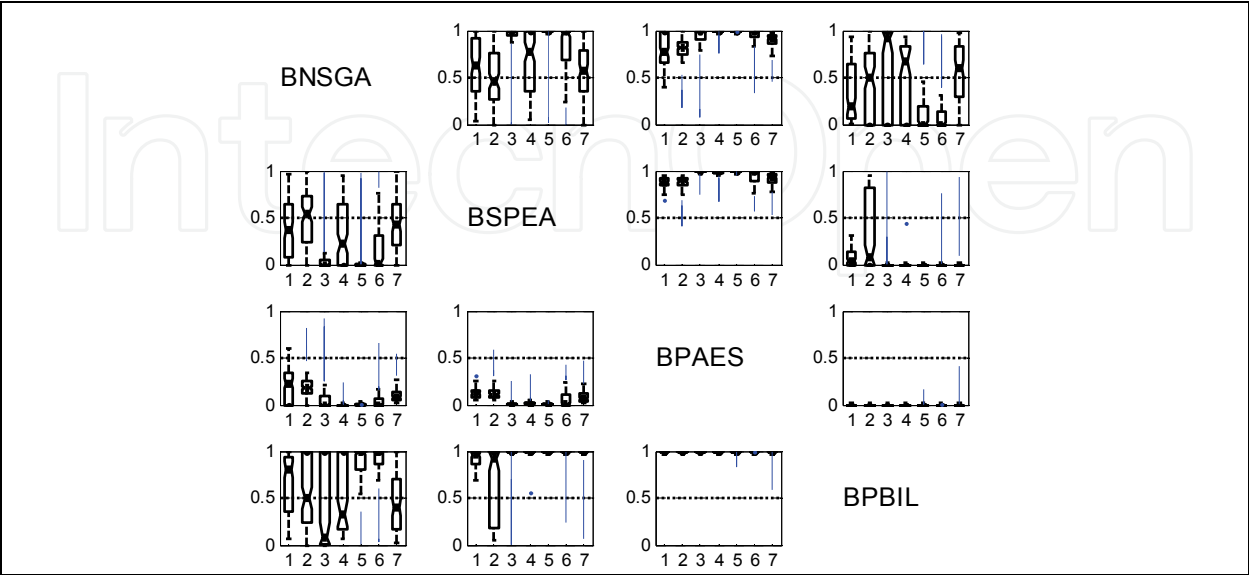Fig. 14. Box-plot of C indicator of ST2 – I

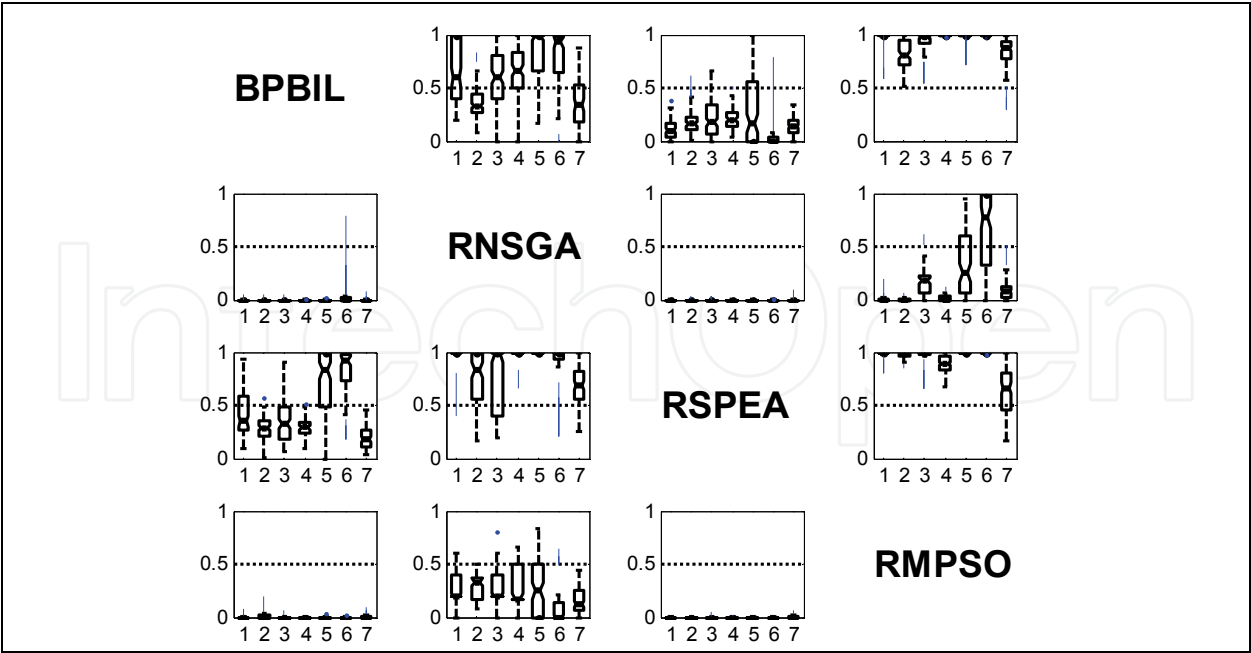Fig. 15. Box-plot of C' indicator of ST2 - I

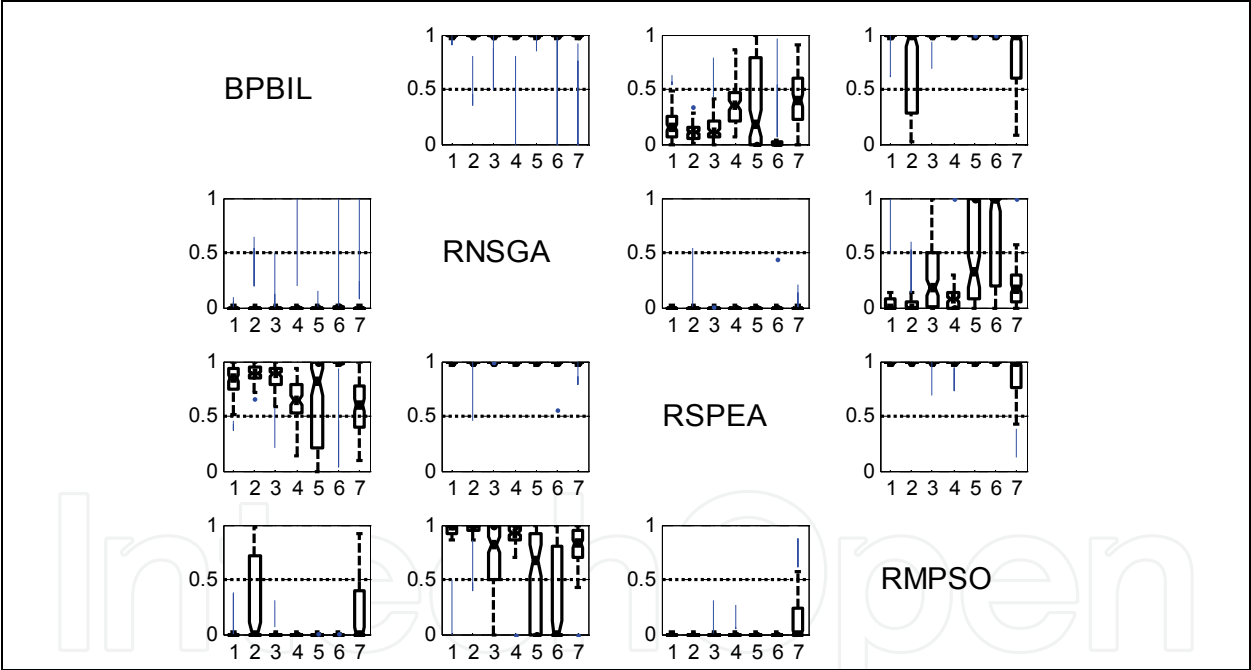Fig. 16. Box-plot of C indicator of ST2 – II

Fig. 17. Box-plot of C' indicator of ST2 - II

The BPBIL algorithm is chosen to solve the P2, P4 and P6 design problems where the structure to be optimised is ST3. In this design case, some structural elements are allowed to be removed if their diameters are too small. The Pareto optimum results of P2 for optimising ST3 obtained from using BPBIL are plotted in Figure 18. Some selected non-dominated solutions are labelled whereas their corresponding structures are given in Figure 19. It can be seen that the structures have various layouts and shapes as well as various element sizes. The approximate Pareto front of P4 is plotted in Figure 20 whereas some selected structures from the front are illustrated in Figure 21. Similarly to the P2 design case, there consist of

Simultaneous Topology, Shape and Sizing Optimisation of Skeletal Structures
Using Multiobjective Evolutionary Algorithms

503

various structural topologies, shape and element sizes. The non-dominated front of P6 obtained from using BPBIL is given in Figure 22 whilst the selected solutions are shown in Figure 23. Similarly to the first two cases, the structures have various topologies, shapes, and element sizes. The obvious advantage of using MOEA for solving the simultaneous topology/shape/sizing optimisation is that they are robust and simple to use, and we can have a set of Pareto optimal solutions for decision making within one simulation run.
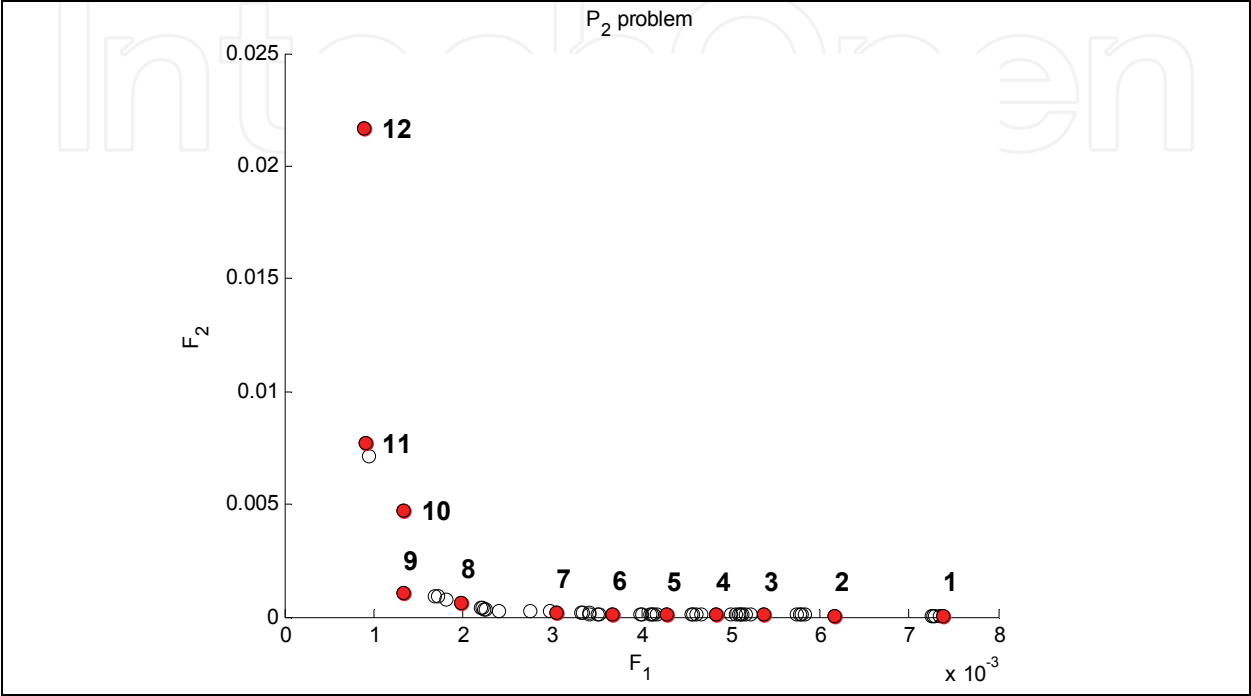
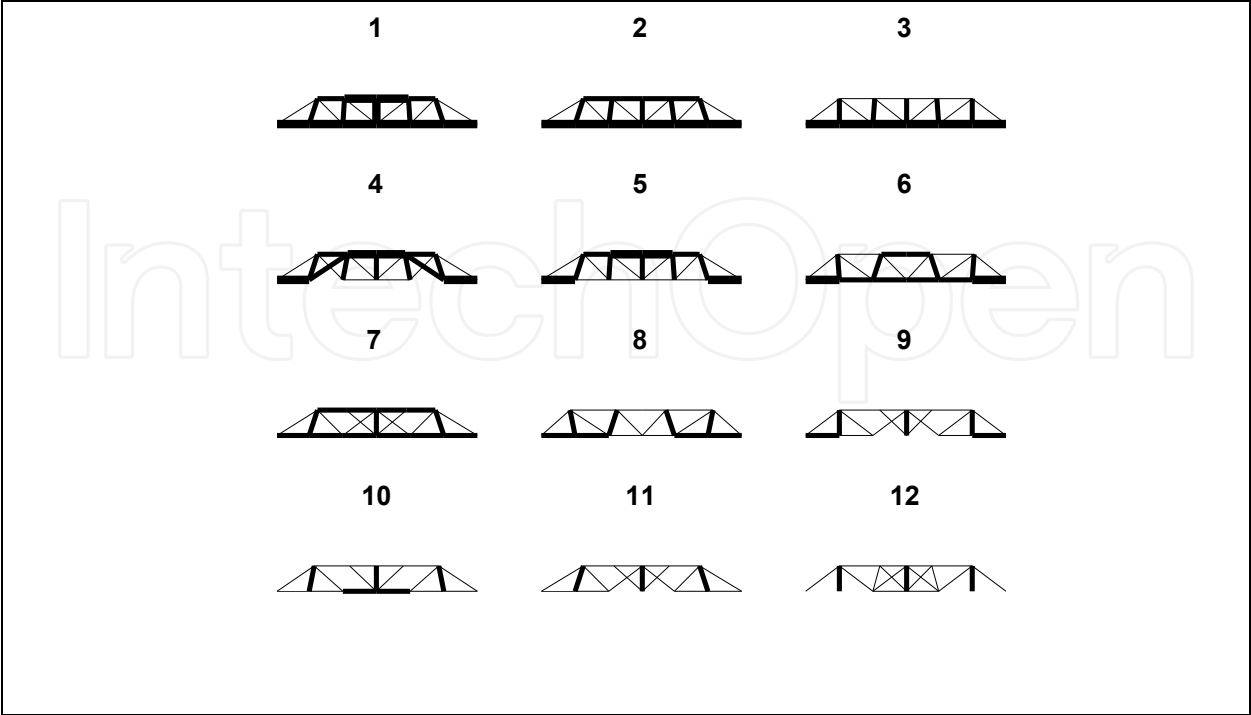Fig. 18. Pareto front of P2 problem and ST3 structures
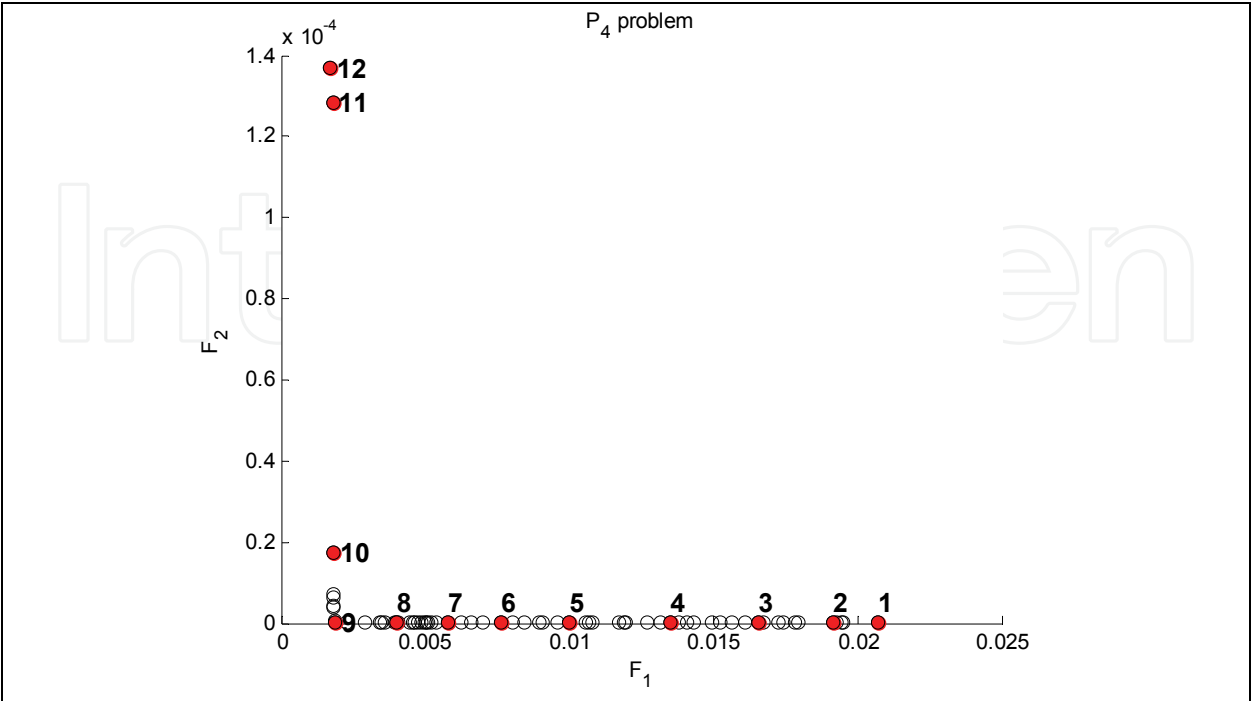

Fig. 19. Some selected structures of P2

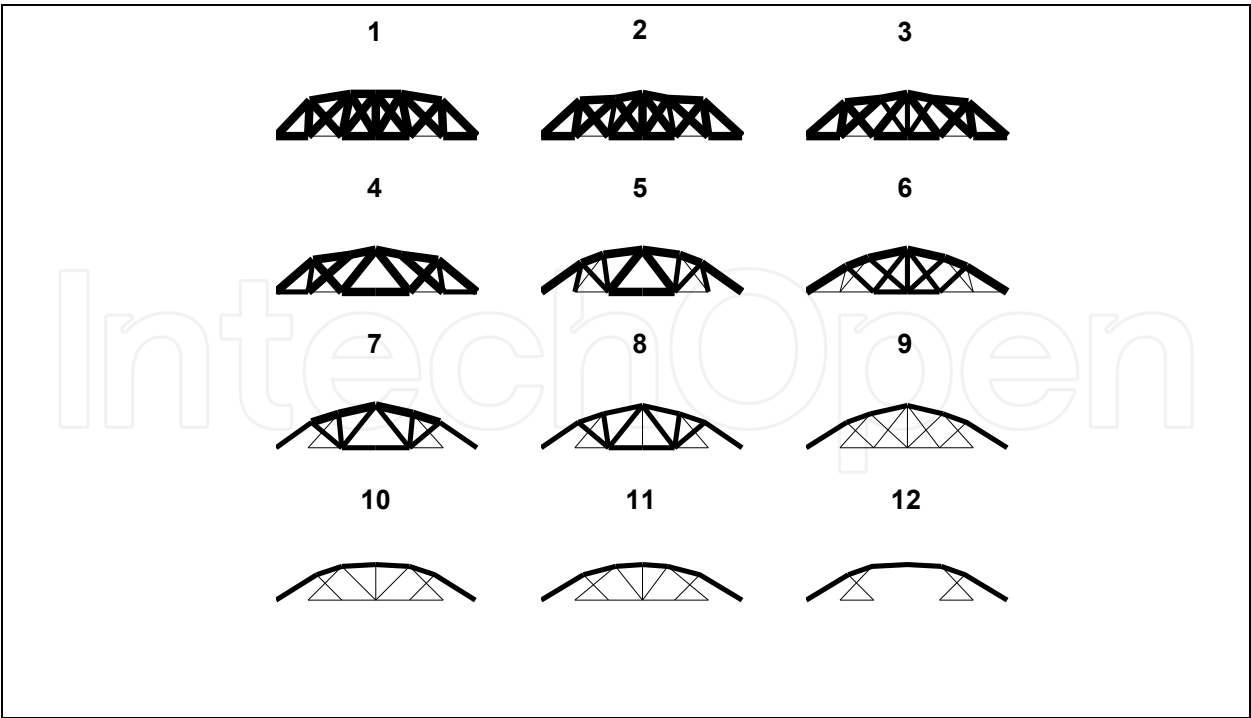Fig. 20. Pareto front of P4 problem and ST3 structures

Fig. 21. Some selected structures of P4

Simultaneous Topology, Shape and Sizing Optimisation of Skeletal Structures
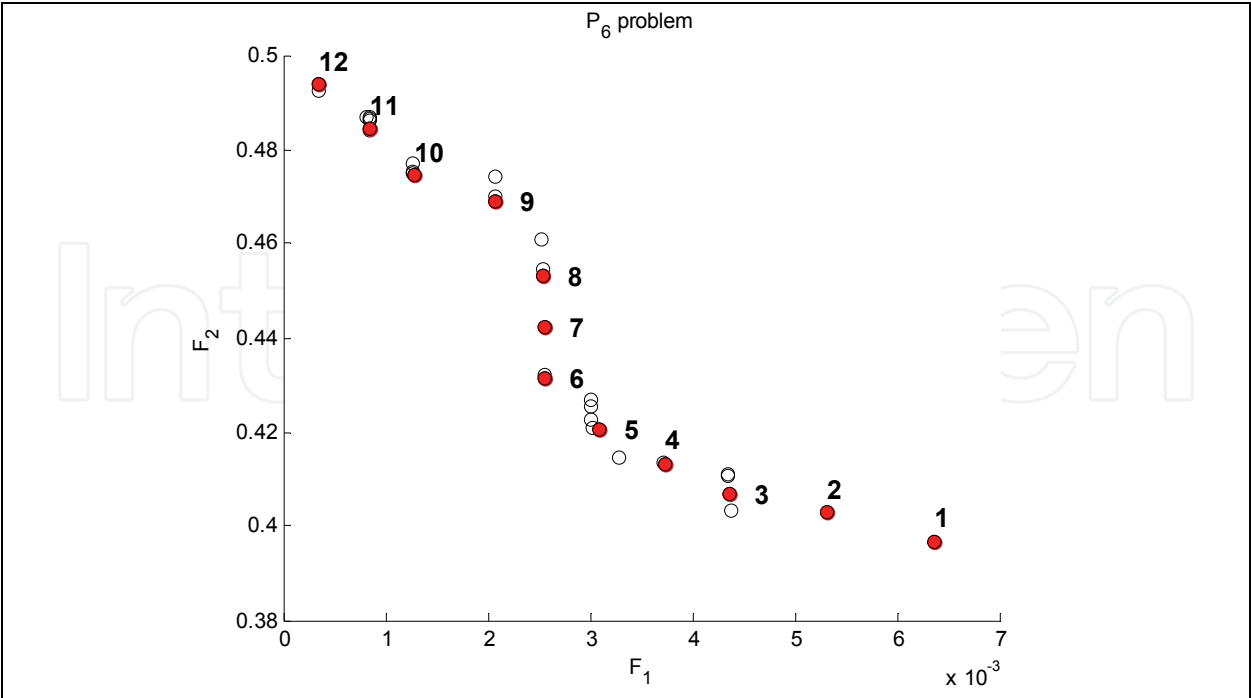Using Multiobjective Evolutionary Algorithms

505

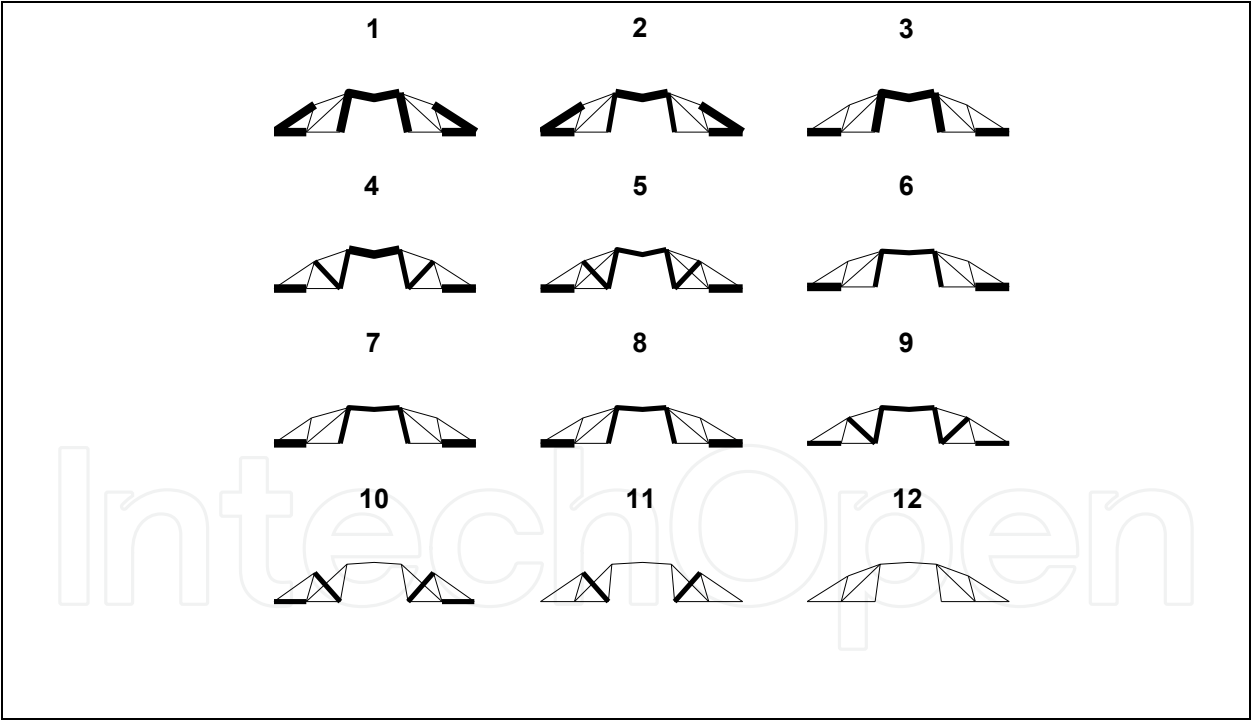Fig. 22. Pareto front of P6 problem and ST3 structures

Fig. 23. Some selected structures of P6

5. Conclusions and discussion

The search procedures of the various MOEAs as well as the static and dynamic analysis of skeletal structures are briefly detailed. Seven multiobjective optimum design problems are posed for benchmarking the performance of the MOEAs. The design problems are applied

to three skeletal structures. The first two structures have simultaneous shape/sizing design variables while the third structure is used for design demonstration of simultaneous topology/shape/sizing optimisation. From the optimum results, it can be concluded that SPEA2 using real codes is the best performer for the ST2 structure which has greater number of design variables. The PBIL using binary string is said to be the best method for ST1, which has a smaller number of design variables. From the design demonstration of using topological, shape, and sizing design variables at the same time, it is shown that BPBIL is an efficient and effective optimisation tool for such a type of structural optimum design. The C and C' indicators should be used together to provide some insight that is missing from using either of them solely. The application of MOEAs for design optimisation of skeletal structures is said to be advantageous since they are robust and simple to use. The method can cope with all kind of design criteria as demonstrated in this work. Most importantly, we can have a set of non-dominated solutions for decision making within one optimisation.

6. References

Achtziger, W. (2007). On simultaneous optimization of truss geometry and topology. *Structural and Multidisciplinary Optimization*, Vol. 33, 285–304

Achtziger, W. & Kocvara, M. (2007). On the maximization of the fundamental eigenvalue in topology optimization. *Structural and Multidisciplinary Optimization*, Vol. 34,181–195

Achtziger, W. & Stolpe, M.(2007). Truss topology optimization with discrete design variables—Guaranteed global optimality and benchmark examples. *Structural and Multidisciplinary Optimization*, Vol. 34,1–20

Alkhatib, R.; Jazar, G. N. & Golnaraghi, M. F. (2004). Optimal design of passive linear suspension using genetic algorithm. *Journal of Sound and Vibration*, Vol. 275, 665-691

Baluja, S. (1994). Population-Based Incremental Learning: A Method for Integrating Genetic Search Based Function Optimization and Competitive Learning. In: *Technical Report CMU_CS_95_163*, School of Computer Science, Carnagie Mellon University, Pittsburgh

Benage, W.A. & Dhingra, A.K. (1994). Single and multiobjective structural optimization in discrete-continuous variables using simulated annealing. *International Journal of Numerical Methods in Engineering*, Vol. 38, 2753-2773

Bureerat, S. & Cooper, J. E. (1998). Evolutionary methods for the optimisation of engineering systems. *IEE Colloquium Optimisation in Control: Methods and Applications*, pp. 1/1-1/10, IEE, London, UK

Bureerat, S. & Sriworamas K. (2007). Population-based incremental learning for multi-objective optimisation. *Advances in Soft Computing*, Vol. 39, 223-232

Chan, C.M. & Wong, K.M. (2008). Structural topology and element sizing design optimization of tall steel frameworks using a hybrid OC–GA method. *Structural and Multidisciplinary Optimization*, Vol. 35, 473–488

Deb, K.; Pratap, A.; Agarwal, S. & Meyarivan, T. (2002). A fast and elitist multiobjective genetic algorithm: NSGAII. IEEE *Transactions on Evolutionary Computation*, Vol. 6, No. 2, 182-197

Deb, K.; Pratap, A. & Meyarivan, T. (2001). Constrained test problems for multi-objective evolutionary optimisation. *Lecture Notes in Computer Science*, Vol. 1993/2001, 284-298

Simultaneous Topology, Shape and Sizing Optimisation of Skeletal Structures
Using Multiobjective Evolutionary Algorithms

507

Hagishita, T. & Ohsaki, M. (2009). Topology optimization of trusses by growing ground structure method. *Structural and Multidisciplinary Optimization*, Vol. 37, 377-393

Hajela, P. & Lee, E. (1995). Genetic algorithms in truss topology optimization. *International Journal of Solids and Structures*, Vol. 32, No. 22, 3341-3357

Hasancebi, O. & Erbatur, F. (2002). Layout optimisation of trusses using simulated annealing. *Advances in Engineering Software*, Vol. 33, 681–696

Kanyakam, S. & Bureerat, S. (2007). Passive vibration suppression of a walking tractor handlebar structure using multiobjective PBIL. *IEEE Congress on Evolutionary Computation (CEC 2007)*, pp. 4162-4169, Singapore

Kawamura, H.; Ohmori, H. & Kito, N. (2002). Truss topology optimization by a modified genetic algorithm. *Structural and Multidisciplinary Optimization*, Vol. 23, 467–472

Keane, A. J. (1995). Passive vibration control via unusual geometries: the applications of genetic algorithm optimization to structural design. *Journal of Sound and Vibration*, Vol. 185, No.30, 441-453

Knowles, J.D. & Corne, D.W. (2000) Approximating the non-dominated front using the Pareto archive evolution strategy. *Evolutionary Computation*, Vol. 8, No. 2, 149-172

Martínez, P.; Martí, P. & Querin, O.M. (2007). Growth method for size, topology, and geometry optimization of truss structures. *Structural and Multidisciplinary Optimization*, Vol. 33, 13–26

Moshrefi-Torbati, M.; Keane, A.J.; Elliott, J.; Brennan, M. J. & Rogers, E. (2003). Passive vibration control of a satellite boom structure by geometric optimization using genetic algorithm, *Journal of Sound and Vibration*, Vol. 276, 879-892.

Noiluplao, C. & Bureerat, S. (2008). Simultaneous topology and shape optimisation of a 3D framework structure using simulated annealing. *Technology and Innovation for Sustainable Development Conference (TISD2008)*, Faculty of Engineering, Khon Kaen University, Thailand, 28-29 January 2008

Ohsaki, M. (1995). Genetic algorithms for topology optimization of trusses. *Computers and Structures*, Vol. 57, No. 2, 219-225

Ohsaki, M. & Katoh, N. (2005). Topology optimization of trusses with stress and local constraints on nodal stability and member intersection. *Structural and Multidisciplinary Optimization*, Vol. 29, 190–197

Preumont, A. (2001). *Vibration control of active structures: an introduction*, Kluwer Academic Publishers

Reyes-Sierra, M. & Coello Coello, C.A.(2006) Multi-objective particle swarm optimizers: a survey of the state-of-the-art. *International Journal of Computational Intelligence Research*, Vol. 2, No. 3, 287-308

Shea, K. & Smith, I.F.C. (2006). Improving full-scale transmission tower design through topology and shape optimization. *Journal of Structural Engineering*, Vol. 132, No. 5, 781–790

Srinivas, N. & Deb, K. (1994). Multiobjective optimization using non-dominated genetic algorithms. *Evolutionary Computation*, Vol. 2, No. 3, 221-248

Srisomporn, S. & Bureerat, S. (2008). Geometrical design of plate-fin heat sinks using hybridization of MOEA and RSM. *IEEE Trans on Components and Packaging Technologies*, Vol. 31, 351-360.

Stolpe, M. & Svanberg, K. (2003). A note on stress-constrained truss topology optimization. *Structural and Multidisciplinary Optimization*, Vol. 25, 62–64

Svanberg, K. & Werme, M. (2007). Sequential integer programming methods for stress constrained topology optimization. *Structural and Multidisciplinary Optimization*, Vol. 34, 277–299

Tang, W.; Tong, L. & Gu, Y. (2005). Improved genetic algorithm for design optimization of truss structures with sizing, shape and topology variables. *International Journal for Numerical Methods in Engineering*, Vol. 62, No. 13, 1737 – 1762

W. H. Tong, J. S. Jiang and G. R. Liu, "Dynamic Design of Structures under Random Excitation," *Computational Mechanics*, vol. 22, 1998, pp. 388-394.

Wang, X.; Wang, M.Y. & Guo, D. (2004). Structural shape and topology optimization in a level-set-based framework of region representation. *Structural and Multidisciplinary Optimization*, Vol. 27, 1–19

Xu, B.; Jiang, J.; Tong, W. & Wu, K. (2003). Topology group concept for truss topology optimization with frequency constraints. *Journal of Sound and Vibration*, Vol. 261, 911–925

Yunkang, S. & Xin, Y. (1998). The topological optimization for truss structures with stress constraints based on the exist-null combined model. *ACTA MECHANICA SINICA (English Series)*, Vol.14, No.4, 363-370

Zhou, M. (1996). Difficulties in truss topology optimization with stress and local buckling constraints. *Structural Optimization*, Vol. 11,134-136

Zhou, M.; Pagaldipti, N.; Thomas, H.L. & Shyy, Y.K. (2004). An integrated approach to topology, sizing, and shape optimization. *Structural and Multidisciplinary Optimization*, Vol. 26, 308–317

Zhu, J.; Zhang, W.; Beckers, P.; Chen, Y. & Guo Z. (2008). Simultaneous design of components layout and supporting structures using coupled shape and topology optimization technique. *Structural and Multidisciplinary Optimization*, Vol. 36, 29–41

Zitzler, E.; Deb, K. & Thiele, L. (2000). Comparison of multiobjective evolutionary algorithms: empirical results. *Evolutionary Computation*, Vol. 8, No. 2, 173-195

Zitzler, E.; Laumanns, M. & Thiele, L. (2002). SPEA2: improving the strength Pareto evolutionary algorithm for multiobjective optimization. *Evolutionary Methods for Design, Optimization and Control*, Barcelona, Spain

Zitzler, E. & Thiele, L. (1999). Multiobjective evolutionary algorithms: a comparative case study and the strength Pareto approach. *IEEE Transactions On Evolutionary Computation*, Vol. 3, No. 4, 257-271

Evolutionary Computation

Edited by Wellington Pinheiro dos Santos

This book presents several recent advances on Evolutionary Computation, specially evolution-based optimization methods and hybrid algorithms for several applications, from optimization and learning to pattern recognition and bioinformatics. This book also presents new algorithms based on several analogies and metafores, where one of them is based on philosophy, specifically on the philosophy of praxis and dialectics. In this book it is also presented interesting applications on bioinformatics, specially the use of particle swarms to discover gene expression patterns in DNA microarrays. Therefore, this book features representative work on the field of evolutionary computation and applied sciences. The intended audience is graduate, undergraduate, researchers, and anyone who wishes to become familiar with the latest research work on this field.

How to reference

In order to correctly reference this scholarly work, feel free to copy and paste the following:

Chaid Noilublao and Sujin Bureerat (2009). Simultaneous Topology, Shape and Sizing Optimisation of Skeletal Structures Using Multiobjective Evolutionary Algorithms, Evolutionary Computation, Wellington Pinheiro dos Santos (Ed.), ISBN: 978-953-307-008-7, InTech, Available from:

http://www.intechopen.com/books/evolutionary-computation/simultaneous-topology-shape-and-sizing-optimisation-of-skeletal-structures-using-multiobjective-evol

INTECH
open science | open minds